

Nonlinear adiabatic passage from fermion atoms to boson molecules

E. Pazy¹, I Tikhonenkov¹, Y. B. Band¹, M. Fleischhauer², and A. Vardi¹

¹*Department of Chemistry, Ben-Gurion University of the Negev, P.O.B. 653, Beer-Sheva 84105, Israel and*

²*Fachbereich Physik, Technische Universität Kaiserslautern, D67663, Kaiserslautern, Germany*

We study the dynamics of an adiabatic sweep through a Feshbach resonance in a quantum gas of fermionic atoms. Analysis of the dynamical equations, supported by mean-field and many-body numerical results, shows that the dependence of the remaining atomic fraction Γ on the sweep rate α varies from exponential Landau-Zener behavior for a single pair of particles to a power-law dependence for large particle number N . The power-law is linear, $\Gamma \propto \alpha$, when the initial molecular fraction is smaller than the $1/N$ quantum fluctuations, and $\Gamma \propto \alpha^{1/3}$ when it is larger. Experimental data agree better with a linear dependence than with an exponential Landau-Zener fit, indicating that many-body effects are significant in the atom-molecule conversion process.

Adiabatic evolution is an important tool for quantum state engineering. The adiabatic theorem ensures that an initial nondegenerate eigenstate remains an instantaneous eigenstate when the Hamiltonian changes slowly. When eigenstates become nearly degenerate, the Landau-Zener (LZ) model [1] is a paradigm for explaining how transitions occur.

Adiabatic sweeps across an atom-molecule Feshbach resonance have recently been used to convert degenerate fermionic atomic gases containing two different internal spin states to bosonic dimer molecules [2, 3, 4, 5]. Formation of a molecular condensate has also been observed using both adiabatic sweeps and three-body recombination processes [6]. In this Letter we show that for adiabatic Feshbach sweeps that convert degenerate fermionic atoms to diatomic molecules, the LZ behavior for a single pair of particles is dramatically changed due to many-body effects. The fraction of unconverted atoms is shown to be a power-law in the sweep rate, rather than exponentially small as predicted by an essentially single-particle, linear LZ model [1, 7]. The exact power-law is determined by the significance of quantum fluctuations. En route to this result we also find that, for a ladder of atomic states filled by fermionic atoms, the atom-molecule sweep efficiency is unaffected by atomic dispersion, and all fermionic atoms can go over to molecules, in contrast to the linear LZ model.

We consider the collisionless, interaction representation, single bosonic mode Hamiltonian [8, 9, 10, 11, 12, 13, 14]

$$H = \sum_{\mathbf{k}, \sigma} \epsilon_{\mathbf{k}} c_{\mathbf{k}, \sigma}^\dagger c_{\mathbf{k}, \sigma} + \mathcal{E}(t) b_0^\dagger b_0 + g \left(\sum_{\mathbf{k}} c_{\mathbf{k}, \uparrow} c_{-\mathbf{k}, \downarrow} b_0^\dagger + H.c. \right), \quad (1)$$

where $\epsilon_{\mathbf{k}} = \hbar^2 k^2 / 2m$ is the kinetic energy of an atom with mass m , and g is the atom-molecule coupling strength. The molecular energy $\mathcal{E}(t) = \alpha t$ is linearly swept at a rate α through resonance to induce adiabatic conversion of Fermi atoms to Bose molecules. The annihilation operators for the atoms, $c_{\mathbf{k}, \sigma}$, obey fermionic anticommutation

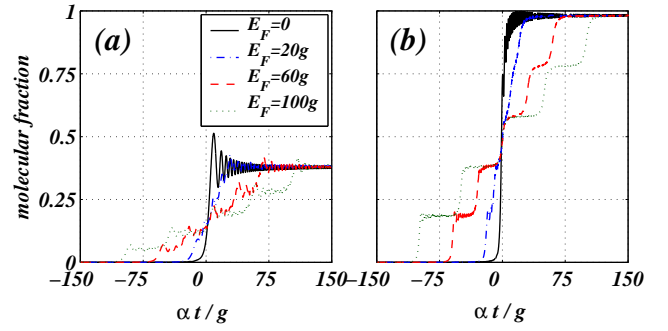


FIG. 1: Many-body collective dynamics of adiabatic passage from a fermionic atomic gas into a molecular BEC for five pairs of fermionic atoms. (a) Sweep rate $\alpha = 2g^2N$, (b) Sweep rate $\alpha = g^2N/4$. Overall efficiency is independent of atomic dispersion in both (a) and (b).

relations, whereas the molecular annihilation operator b_0 obeys a bosonic commutation relation.

We find that, provided that all atomic levels are swept through, the adiabatic conversion efficiency is completely insensitive to the details of the atomic dispersion. Fig. 1 shows exact numerical results for the adiabatic conversion of five atom pairs into molecules, for different values of the atomic level spacing (and hence of the Fermi energy E_F). It is evident that, while the exact dynamics depends on E_F , levels are sequentially crossed, leading to the same final efficiency regardless of the atomic motional timescale. In particular, in the limit as $\alpha \rightarrow 0$ it is possible to convert *all* atom pairs into molecules. This is a unique feature of the nonlinear parametric coupling between atoms and molecules, which should be contrasted with a marginal conversion efficiency expected for linear coupling. Since the exact energies $\epsilon_{\mathbf{k}}$ do not affect the final fraction of molecules, we use a degenerate model [12, 13, 14] with $\epsilon_{\mathbf{k}} = \epsilon$ for all \mathbf{k} . In the spirit of Refs. [13, 15], we define the operators:

$$\mathcal{J}_- = \frac{b_0^\dagger \sum_{\mathbf{k}} c_{\mathbf{k}, \uparrow} c_{-\mathbf{k}, \downarrow}}{(N/2)^{3/2}}, \quad \mathcal{J}_+ = \frac{\sum_{\mathbf{k}} c_{-\mathbf{k}, \downarrow}^\dagger c_{\mathbf{k}, \uparrow}^\dagger b_0}{(N/2)^{3/2}},$$

$$\mathcal{J}_z = \frac{\sum_{\mathbf{k},\sigma} c_{\mathbf{k},\sigma}^\dagger c_{\mathbf{k},\sigma} - 2b_0^\dagger b_0}{N}, \quad (2)$$

where $N = 2b_0^\dagger b_0 + \sum_{\mathbf{k},\sigma} c_{\mathbf{k},\sigma}^\dagger c_{\mathbf{k},\sigma}$ is the conserved total number of particles. It is important to note that $\mathcal{J}_-, \mathcal{J}_+, \mathcal{J}_z$ do not span $SU(2)$ as $[\mathcal{J}_+, \mathcal{J}_-]$ is a quadratic polynomial in \mathcal{J}_z . We also define $\mathcal{J}_x = \mathcal{J}_+ + \mathcal{J}_-$ and $\mathcal{J}_y = -i(\mathcal{J}_+ - \mathcal{J}_-)$. Up to a c -number term, Hamiltonian (1) takes the form

$$H = \frac{N}{2} \left(\Delta(t) \mathcal{J}_z + g \sqrt{\frac{N}{2}} \mathcal{J}_x \right), \quad (3)$$

where $\Delta(t) = 2\epsilon - \mathcal{E}(t)$. Defining a rescaled time $\tau = \sqrt{N}gt$, we obtain the Heisenberg equations of motion for the association of a quantum-degenerate gas of fermions,

$$\begin{aligned} \frac{d}{d\tau} \mathcal{J}_x &= \delta(\tau) \mathcal{J}_y \\ \frac{d}{d\tau} \mathcal{J}_y &= -\delta(\tau) \mathcal{J}_x + \frac{3\sqrt{2}}{4} (\mathcal{J}_z - 1) \left(\mathcal{J}_z + \frac{1}{3} \right) \\ &\quad - \frac{\sqrt{2}}{N} (1 + \mathcal{J}_z), \\ \frac{d}{d\tau} \mathcal{J}_z &= \sqrt{2} \mathcal{J}_y, \end{aligned} \quad (4)$$

which depend on the single parameter $\delta(\tau) = \Delta(t)/\sqrt{N}g = (\alpha/g^2N)\tau$. We note parenthetically that precisely the same set of equations, with $\mathcal{J}_z \rightarrow -\mathcal{J}_z$ and $g \rightarrow g/2$, is obtained for a two-mode atom-molecule BEC [15], providing another perspective on the recently observed mapping between the two systems [12, 13, 14].

We first consider the mean-field limit of Eqs. (4), replacing $\mathcal{J}_x, \mathcal{J}_y$, and \mathcal{J}_z by their expectation values u , v , and w which correspond to the real and imaginary parts of the atom-molecule coherence and the atom-molecule population imbalance, respectively, and omitting the quantum noise term $\sqrt{2}(1+\mathcal{J}_z)/N$. In this limit, the equations depict the motion of a generalized Bloch vector on a two-dimensional surface, determined by the conservation law,

$$u^2 + v^2 = \frac{1}{2}(w-1)^2(w+1). \quad (5)$$

Hamiltonian (3) is then replaced by the classical form

$$H(w, \theta; \Delta) = \frac{gN^{3/2}}{2} \left(\delta w + \sqrt{(1+w)(1-w^2)} \cos \theta \right), \quad (6)$$

with $\theta = \arctan(v/u)$.

To study the atom-molecule adiabatic passage, we closely follow the method of Ref. [16]. The eigenvalues of the atom-molecule system at any given value of δ correspond to the fixed points (u_0, v_0, w_0) of the classical Hamiltonian (6) or the mean-field limit of Eqs. (4):

$$v_0 = 0, \quad \frac{\sqrt{2}}{4} (w_0 - 1) (3w_0 + 1) = \delta u_0. \quad (7)$$

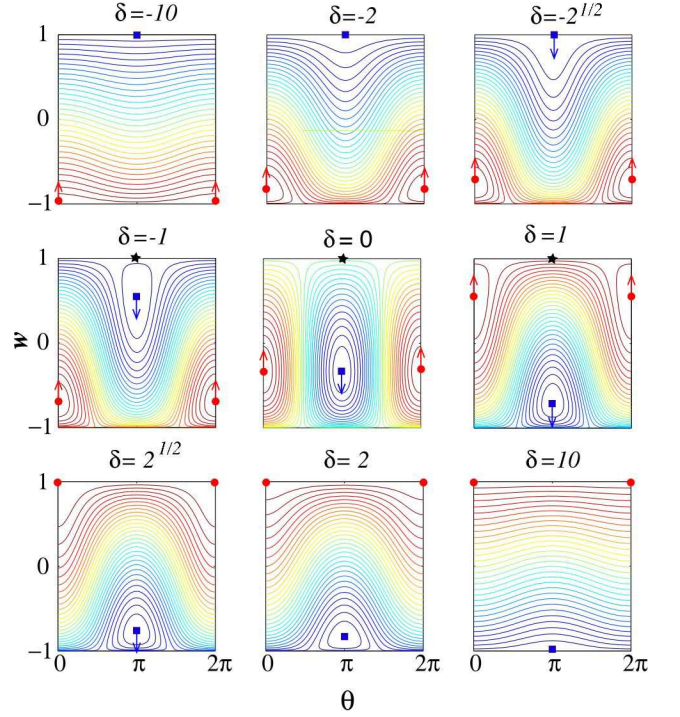


FIG. 2: Equal-energy contours of Hamiltonian (6) plotted as a function of w and θ for different detunings δ . $w = 1$ is all atoms and $w = -1$ is all molecules. The various fixed points corresponding to adiabatic eigenvectors are marked by (blue) squares, (red) circles and (black) stars.

The number of fixed points depends on the parameter δ . The point $u_0 = v_0 = 0, w_0 = 1$ is stationary for any value of δ . Using Eqs. (5) and (7), other fixed points satisfy

$$\frac{(3w_0 + 1)^2}{4(w_0 + 1)} = \delta^2. \quad (8)$$

In Fig. 2 we plot phase-space trajectories, corresponding to equal-energy contours of Hamiltonian (6), for different values of δ . As expected from (6), the plots have the symmetry $(w, \theta; \delta) \leftrightarrow (w, \theta + \pi; -\delta)$. For sufficiently large detuning, $|\delta| > \sqrt{2}$, Eq. (8) has only one solution in the range $-1 \leq w_0 \leq 1$. Therefore, there are only two (elliptic) fixed points, denoted by a red circle corresponding to the solution of Eq. (8), and a blue square at $(0,0,1)$. As the detuning is changed, one of these fixed points (red circle) smoothly moves from all-molecules towards the atomic mode. At detuning $\delta = -\sqrt{2}$ a homoclinic orbit appears through the point $(0,0,1)$ which bifurcates into an unstable (hyperbolic) fixed point (black star) remaining on the atomic mode, and an elliptic fixed point (blue square) which starts moving towards the molecular mode. Consequently, in the regime $|\delta| < \sqrt{2}$ there are two elliptic fixed points and one hyperbolic fixed point, corresponding to the unstable all-atoms mode. Another crossing occurs at $\delta = \sqrt{2}$ when the fixed point which started near the molecular mode (red circle) coalesces with the all-atoms mode (black star).

The frequency of small periodic orbits around the fixed points, Ω_0 , is found by linearization of the dynamical equations (4) about (u_0, v_0, w_0) and using (8) to obtain

$$\frac{\Omega_0}{g\sqrt{N}} = \sqrt{\delta^2 + (1 - 3w_0)} = \sqrt{\frac{(1 - w_0)(3w_0 + 5)}{4(w_0 + 1)}}. \quad (9)$$

Hence, for $|\delta| < \sqrt{2}$ the period of the homoclinic trajectory beginning at $(0, 0, 1)$ diverges.

Transforming w, θ into action-angle variables I, ϕ , the non-adiabatic tunneling probability Γ at any finite sweep rate α is related to the action I accumulated during the sweep [1, 16, 17],

$$\Gamma^2 = \frac{\Delta I}{2} = \frac{1}{2} \int_{-\infty}^{\infty} R(I, \phi) \dot{\Delta} \frac{d\phi}{\dot{\phi}}, \quad (10)$$

where $R(I, \phi)$ is related to the generating function of the canonical transformation $w, \theta \rightarrow I, \phi$. We note that, unlike the linear [1] or Josephson [16, 17] case, where the tunneling probability is linearly proportional to the action increment ΔI , our choice of variables (2) causes the atomic population at the end of the sweep (and hence, Γ) to be proportional to the *square root* of ΔI (since $u^2(t_f) + v^2(t_f) \propto \left| \sum_{\mathbf{k}, \sigma} n_{\mathbf{k}, \sigma}(t_f) \right|^2$, where $n_{\mathbf{k}, \sigma}(t_f)$ is the population in state $|\mathbf{k}, \sigma\rangle$ at the final time t_f). Equation (10) depicts the familiar rule that in order to attain adiabaticity, the rate of change of the adiabatic fixed points through the variation of the adiabatic parameter Δ , $R(I, \phi) \dot{\Delta}$, should be slow with respect to the characteristic precession frequency $\dot{\phi} = \Omega_0$ about these stationary vectors. For an adiabatic process where $\dot{\Delta}/\dot{\phi} \rightarrow 0$, the action (which is proportional to the surface-area enclosed within the periodic orbit) is an adiabatic invariant, so a zero-action elliptic fixed point evolves into a similar point trajectory. Action is accumulated mainly in the vicinity of singularities where $\dot{\phi} = \Omega_0 \rightarrow 0$. For linear adiabatic passage [1], such singular points lie exclusively off the real axis, leading to exponential LZ transition probabilities. However, when nonlinearities are dominant, as in the Mott-insulating Josephson case [16, 17] and our case, there are real singularities, leading to power-law dependence of the transfer efficiency on the sweep rate.

It is clear from Eq. (9) that, for the atom-molecule conversion problem, a real singularity of the integrand in Eq. (10) exists at $w_0 = 1$, where the frequency vanishes as $\Omega_0 \approx g\sqrt{N(1 - w_0)}$. Thus, most the the nonadiabatic correction is accumulated in the vicinity of this point (all-atoms for fermions and all-molecules for bosons). Taking the derivative of Eq. (8) with respect to time, we find that the response of the fixed-point velocity to a linear sweep rate α is,

$$\dot{w}_0 = \frac{4\alpha}{g\sqrt{N}} \frac{(w_0 + 1)^{3/2}}{3w_0 + 5}. \quad (11)$$

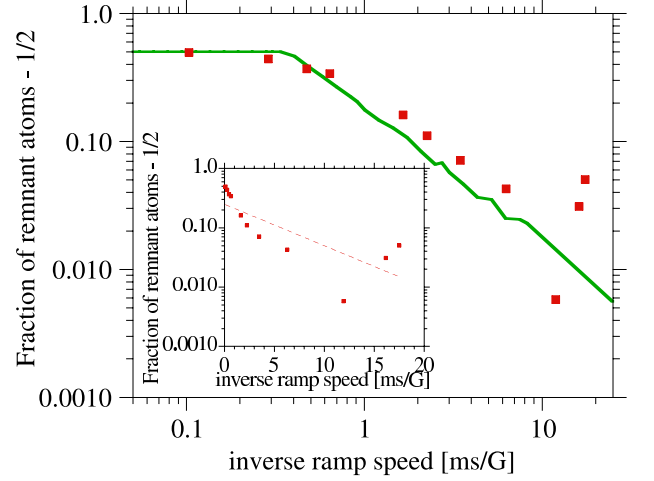


FIG. 3: Fraction of remnant atoms versus inverse ramp speed $1/\dot{B}$ across the 543 G resonance in a two-component Fermi gas of ^6Li . The experimental data (red squares) of Ref. [3], which saturates at a remnant of $1/2$ [20], and the mean-field calculations obey a linear dependence on sweep rate beyond 0.4 ms/G . $\frac{\alpha^2}{N}$ is multiplied by 0.4 ms/G to scale the abscissa for the calculated results. The insert shows the best exponential fit of the data as a dashed line.

Having found \dot{w}_0 , we can now find the action-angle variable ϕ in terms of w_0 : $\phi = \int \dot{\phi} dt = \int \Omega_0 \frac{dw_0}{\dot{w}_0}$. In the vicinity of the singularity we have $\Omega_0 \approx g\sqrt{N(1 - w_0)}$ and $\dot{w}_0 \approx \sqrt{2}\alpha/g\sqrt{N}$, resulting in

$$\phi = \frac{g^2 N}{\alpha} \frac{\sqrt{2}}{3} (1 - w_0)^{3/2}. \quad (12)$$

Using Eq. (12), we finally find that near the singularity, $\dot{\phi} = \Omega_0 \approx g\sqrt{N(1 - w_0)}$ is given in terms of ϕ as

$$\dot{\phi} = \left(3\sqrt{\frac{N}{2}} g \alpha \right)^{1/3} \phi^{1/3}. \quad (13)$$

Substituting (13) and $\dot{\Delta} = \alpha$ into Eq. (10) we find that the nonadiabatic correction depends on α as

$$\Gamma \propto \alpha^{1/3}. \quad (14)$$

So far, we have neglected the effect of quantum fluctuations, which are partially accounted for by the source term $(\sqrt{2}/N)(1 + \mathcal{J}_z)$ in Eqs. (4). As a result, we found that \dot{w}_0 does not vanish as w_0 approaches 1. Consequently, the remaining atomic population is expected to scale as the cubic root of the sweep rate if the initial average molecular fraction is larger than the quantum noise. However, starting purely with fermion atoms (or with molecules made of bosonic atoms), fluctuations will initially dominate the conversion process. Equation (8) should then be replaced by

$$\delta = \frac{2}{\sqrt{w_0 + 1}} \left(\frac{3w_0 + 1}{4} - \frac{w_0 + 1}{N(w_0 - 1)} \right), \quad (15)$$

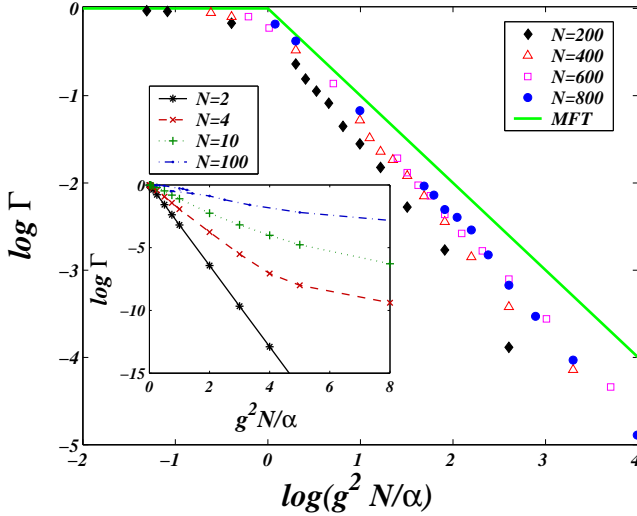


FIG. 4: Many-body calculations for the fraction of remnant atoms versus dimensionless inverse sweep rate for various particle numbers in the range $N = 2$ to 800. The many body results for large number of particles converge to the mean-field results (solid green line) of Fig. 3.

demonstrating that our previous treatment around $w_0 = 1$ is only valid provided that $|w_0(t_i) - 1| \gg 1/N$. For smaller initial molecular population, Eq. (11) should be replaced by

$$\dot{w}_0 = \frac{\alpha}{g\sqrt{N}} \left/ \left[\frac{3w_0 + 5}{4(w_0 + 1)^{3/2}} + \frac{w_0 + 3}{N(w_0 + 1)^{1/2}(w_0 - 1)^2} \right] \right. \quad (16)$$

Hence, in the vicinity of $w_0 = 1$ the eigenvector velocity in the w direction vanishes as $\dot{w}_0 = (\sqrt{N}\alpha/g\sqrt{8})(w_0 - 1)^2$. The characteristic frequency $\dot{\phi}$ is now proportional to $(\alpha\phi)^{-1}$ instead of Eq. (13) so that $\Delta I \propto \alpha^2$, and [18, 19]

$$\Gamma \propto \alpha. \quad (17)$$

Equations (17) and (14) constitute the main results of this work. We predict that the remnant atomic fraction in adiabatic Feshbach sweep experiments will scale as a power-law with sweep rate due to the curve crossing in the nonlinear case. The dependence is expected to be linear if the initial molecular population is below the quantum-noise level (i.e., when $1 - w_0(t_i) \ll 1/N$), and cubic-root when fluctuations can be neglected (i.e. for $1 - w_0(t_i) \gg 1/N$). We note that a similar linear dependence was predicted for adiabatic passage from bosonic atoms into a molecular BEC [18].

The analytical predictions illustrated above are confirmed by numerical simulations and existing experimental data. Fig. 3 shows the fraction of remnant atoms Γ versus inverse sweep rate $\frac{g^2}{\alpha N}$, computed numerically from the mean-field limit of Eqs. (4). The log-log plot highlights the power law dependence obtained beyond

0.4 ms/G (i.e., for $\frac{g^2}{\alpha N} > 1$). The numerical results compare quite well with the experimental data of Ref. [3] (red squares in Fig. 3), indicating that nonlinear effects do indeed dominate the adiabatic passage dynamics in these experiments. The power-law fit of the experimental results is contrasted with an exponential LZ fit (insert of Fig. 3) which fails to provide an accurate description of the observed dependence of efficiency on sweep rate.

To go beyond the mean-field analysis we carry out exact many-body calculations of efficiency vs. dimensionless inverse sweep-rate, $\frac{g^2}{\alpha N}$, using the methodology of [12]. The results are shown in Fig. 4. For a single pair of particles, $N = 2$, the quantum association problem is formally identical to the linear LZ paradigm, leading to an exponential dependence of the remnant atomic fraction on sweep rate (see insert of Fig. 4). However, as the number of particles increases, many-body effects come into play, and there is a smooth transition to a power-law behavior in the regime $\alpha < g^2 N$. We note that this is precisely the regime where Eq. (10) can be used to estimate ΔI and Γ [1].

In summary, we have shown that nonlinear many-body effects play a significant role in the atom-molecule conversion process for degenerate fermionic atomic gases, modifying the LZ exponential dependence on sweep rate. Experimental data seem to back up this conclusion.

This work was supported in part by grants from the U.S.-Israel Binational Science Foundation (grant Nos. 2002214, 2002147), the Minerva Foundation through a grant for a Minerva Junior Research Group, the Israel Science Foundation for a Center of Excellence (grant No. 8006/03), and the German Federal Ministry of Education and Research (BMBF) through the DIP project.

-
- [1] L. D. Landau, Phys. Z. Sowjetunion **2**, 46 (1932); G. Zener, Proc. R. Soc. London, Ser. A **137**, 696 (1932); L. D. Landau and E. M. Lifshitz, *Mechanics* (Pergamon, Oxford, 1976), Sec. 51.
 - [2] C. A. Regal *et al.*, Nature (London) **424**, 47 (2003).
 - [3] K. E. Strecker *et al.*, Phys. Rev. Lett. **91**, 080406 (2003).
 - [4] J. Cubizolles *et al.*, Phys. Rev. Lett. **91**, 240401 (2003).
 - [5] E. Hodby *et al.*, cond-mat/0411487.
 - [6] M. Greiner *et al.*, Nature (London) **426**, 537 (2003); S. Jochim *et al.*, Science **302**, 2101 (2003); M.W. Zwierlein *et al.*, Phys. Rev. Lett. **91**, 250401 (2003).
 - [7] F. H. Mies *et al.*, Phys. Rev. A **61**, 022721 (2000); K. Góral *et al.*, J. Phys. B **37**, 3457 (2004); J. Chwedeńczuk *et al.*, Phys. Rev. Lett. **93**, 260403 (2004).
 - [8] J. Javanainen *et al.*, Phys. Rev. Lett. **92**, 200402 (2004).
 - [9] R. A. Barankov and L. S. Levitov, Phys. Rev. Lett. **93**, 130403 (2004).
 - [10] A. V. Andreev *et al.*, Phys. Rev. Lett. **93**, 130402 (2004).
 - [11] J. Dukelsky *et al.*, Phys. Rev. Lett. **93**, 050403 (2004).
 - [12] I. Tikhonenkov and A. Vardi, cond-mat/0407424.
 - [13] T. Miyakawa and P. Meystre, cond-mat/0409689.

- [14] M. Mackie and O. Dannenberg, physics/0412048.
- [15] A. Vardi *et al.*, Phys. Rev. A **64**, 063611 (2001).
- [16] J. Liu *et al.*, Phys. Rev. A **66**, 023404 (2002).
- [17] O. Zobay and B. M. Garraway, Phys. Rev. A **61**, 033603 (2000).
- [18] A. Ishkhanyan *et al.*, Phys. Rev. A **69**043612 (2004).
- [19] E. Altman and A. Vishwanath, cond-mat/0501683.
- [20] E. Pazy *et al.*, Phys. Rev. Lett. **93**, 120409 (2004).